THE JOURNAL OF PHYSICAL CHEMISTRY A

Article

pubs.acs.org/JPCA

Sensitivity and Selectivity of Switchable Reagent Ion Soft Chemical Ionization Mass Spectrometry for the Detection of Picric Acid

Bishu Agarwal,[†,‡] Ramón González-Méndez,[§] Matteo Lanza,[†] Philipp Sulzer,[†] Tilmann D. Märk,[†,‡] Neil Thomas,[§] and Chris A. Mayhew*[,§]

[†]IONICON Analytik Gesellschaft m.b.H., Eduard-Bodem-Gasse 3, A-6020 Innsbruck, Austria

[‡]Institut für Ionenphysik und Angewandte Physik, Leopold-Franzens-Universität Innsbruck, Technikerstr. 25, A-6020 Innsbruck, Austria

[§]School of Physics and Astronomy, University of Birmingham, Edgbaston, Birmingham, B15 2TT, U.K.

ABSTRACT: We have investigated the reactions of NO^+, H_3O^+, O_2^+, and Kr^+ with picric acid (2,4,6 trinitrophenol, $C_6H_3N_3O_7$, PiA) using a time-of-flight mass spectrometer with a switchable reagent ion source. NO^+ forms a simple adduct ion PiA·NO^+, while H_3O^+ reacts with PiA via nondissociative proton transfer to form $PiAH^+$. In contrast, both O_2^+ and Kr^+ react with PiA by nondissociative charge transfer to produce PiA^+. For Kr^+, we also observe dissociation of PiA, producing NO_2^+ with a branching percentage of approximately 40%. For the reagent ions H_3O^+ and O_2^+ (and operating the drift tube with normal laboratory air), we find that the intensities of the $PiAH^+$ and PiA^+ ions both exhibit a peak at a given drift-tube voltage (which is humidity dependent). This unusual behavior implies a peak in the detection sensitivity of PiA as a function of the drift-tube voltage (and hence E/N). Aided by electronic-structure calculations and our previous studies of trinitrotoluene and trinitrobenzene, we provide a possible explanation for the observed peak in the detection sensitivity of PiA.

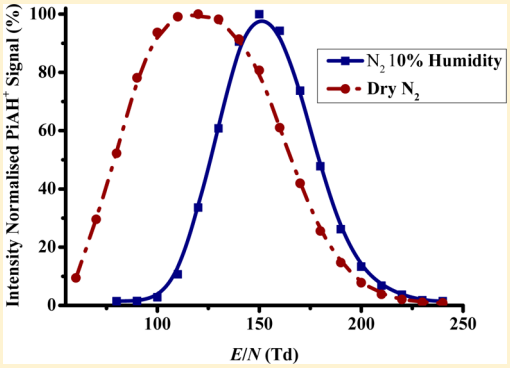

INTRODUCTION

A number of our recent publications have demonstrated the use of switchable reagent ion soft chemical ionization mass spectrometric instrumentation for the detection of various threat agents including explosives,[1−5] drugs,[4,6−9] chemical warfare agents,[10,11] and toxic industrial compounds.[11] The explosive studies have included the reactions of H_3O^+ with trinitrotoluene (TNT), trinitrobenzene (TNB), pentaerythritol tetranitrate (PETN), cyclotrimethylenetrinitramine (RDX), 1,3-dinitrobenzene (DNB), and 2,4-dinitrotoluene (DNT),[1−4] and O_2^+ and NO^+ with TNT, TNB, PETN, and RDX.[5] The aim of our studies into different reagent ions is to investigate whether rapid switching between them could enhance the selectivity of detection, i.e., whether it is possible to distinguish isobaric and isomeric compounds.

A particularly interesting finding from the H_3O^+ studies with explosives was the dependence of the detection sensitivity of $TNTH^+$ and $TNBH^+$ on reduced electric field (the ratio of the electric field strength E and the gas number density N in the drift tube).[3] For the majority of PTR-MS studies, it has been found that the signal intensity for the protonated parent decreases with increasing E/N (e.g., in the case of the explosives, this is observed to occur dramatically for RDX and PETN). A decrease in the protonated parent ion signal with increasing E/N is the expected behavior owing to reduced reaction times and increased collisional induced dissociation. A decrease in the protonated parent ion signal is also observed for low E/N if association of the protonated parent with water present in the drift tube occurs. If this association occurs at a given E/N, then it will be observed that the protonated signal intensity would initially increase as E/N is increased owing to the reduction in association, reach a maximum, and then begin to decrease owing to the two factors already mentioned above. It can normally be expected that any decrease with the protonated parent (MH^+) as a result of association with water would be mirrored by an increase in the $MH^+·H_2O$ signal intensity, so that the parent molecule of interest would still be involved in a product ion (e.g., this has been observed for 1,3-DNB and 2,4-DNT),[3] and hence an identifiable m/z in the mass spectrum. However, this is not always the case. For $TNTH^+$ and $TNBH^+$, no significant increase in the $MH^+·H_2O$ ion signals was observed at low E/N because of a ligand switching process:

$$MH^+·H_2O + H_2O \rightarrow H_3O^+·H_2O + M \quad (1)$$

Given that the terminal ion does not contain the explosive and is one that is already abundant in the drift tube so that the contribution from the secondary reactions cannot be detected,

Special Issue: A. W. Castleman, Jr. Festschrift

Received: January 29, 2014
Revised: February 21, 2014
Published: February 21, 2014

dx.doi.org/10.1021/jp5010192 | J. Phys. Chem. A 2014, 118, 8229−8236

Table 1. Enthalpy and Free Energy Changes for the Reactions of H_3O^+, $H_3O^+{\cdot}H_2O$, and $H_3O^+{\cdot}2H_2O$ with Picric Acid (PiA) at 298 K Calculated at the B3LYP 6-31+G(d,p) Level

reactants	product(s)	ΔH_{298} (kJ mol^{-1})	ΔG_{298} (kJ mol^{-1})
PiA + H_3O^+	PiA1H$^+{\cdot}H_2O$	−139	−97
	PiA1H$^+$ + H_2O	−80	−75
	PiA4H$^+{\cdot}H_2O$	−124	−86
	PiA4H$^+$ + H_2O	−27	−27
PiA + $H_3O^+{\cdot}H_2O$	PiA1H$^+{\cdot}2H_2O$	−66	−27
	PiA1H$^+{\cdot}H_2O$ + H_2O	+19	+27
	PiA4H$^+{\cdot}2H_2O$	−74	−28
	PiA4H$^+{\cdot}H_2O$ + H_2O	+34	+37
PiA + $H_3O^+{\cdot}2H_2O$	PiA1H$^+{\cdot}3H_2O$	−58	−11
	PiA1H$^+{\cdot}2H_2O$ + H_2O	+29	+37
	PiA4H$^+{\cdot}3H_2O$	−55	−7
	PiA4H$^+{\cdot}2H_2O$ + H_2O	+21	+37

reaction 1 results in a loss of sensitivity for the detection of TNTH$^+$ and TNBH$^+$ as E/N is reduced.

Reaction 1 is not common, and an aim of our recent studies has been to investigate whether any other explosives or explosive related compounds behave in a similar fashion. The importance of this relates to the appropriate conditions needed to enhance sensitivity (correct E/N) and selectivity (rapid switching of E/N) of detection. Therefore, we have investigated a large number of compounds, including nitrobenzene, nitromethane, nitrotoluenes, dinitrobenzenes, dinitrotoluenes, and picric acid (PiA). Only the trinitroaromatic compound picric acid ($C_6H_3N_3O_7$) was found to behave in a similar way to TNT and TNB, and this compound is therefore the subject of this paper.

In addition to using H_3O^+ as a reagent ion, in this study, we have extended this investigation by looking at the reaction of picric acid with NO^+, O_2^+, and Kr^+ to determine what product ions are produced, so that we can not only determine if selectivity can be enhanced for picric acid detection by switching the reagent ions but also investigate the sensitivity of detection as a function of E/N for these three reagent ions. Of particular interest here is that we have found that the intensity of the product ion resulting from the reaction of O_2^+ with picric acid behaves in a similar way to that observed for protonated picric acid with E/N, although over a different E/N range.

To aid in the interpretation of the experimental results, DFT calculations have been undertaken to determine theromochemical values for picric acid and its reaction with various ions. These calculations are also reported in this paper.

EXPERIMENTAL AND THEORETICAL DETAILS

Electronic Structure Calculations. Density functional theory calculations using the Gaussian 09 program with the GaussView 5 interface have been undertaken to determine the proton affinity of picric acid, heats of formation of various ions, and reaction processes at 298 K.[12] Although it is appreciated that the drift tube temperature used in our experiments is greater than 298 K, the thermochemical calculations at 298 K provide a useful indication as to whether a reaction pathway is energetically possible or not. The B3LYP functional with the 6-31+G(d,p) basis set was used for this study.

Experimental Methods. For this study, we have used the recently developed switchable reagent ion PTR-TOF 8000 (manufactured by Ionicon Analytik GmbH, Austria).[13] A full description of this instrument has already been published,[14] and hence, only brief details will be provided here.

Carrier gas was passed through a septum into a glass vial containing picric acid. The carrier gas passed over the sample and was drawn into a tube connected to the inlet system of the PTR-TOF 8000. The glass vial was kept at approximately 70 °C, whereas the sample inlet line and the drift tube were maintained at approximately 120 °C. For those H_3O^+ and O_2^+ experiments where we wished to keep the humidity in the drift tube to a minimum value, high purity nitrogen was used as a carrier gas; otherwise, normal laboratory air was used after it had been passed through a hydrocarbon trap. For the Kr^+ experiments, the drift tube was operated under extremely dry conditions (defined as the case when the H_3O^+ signal intensity is less than approximately 3% of the total Kr^+ ion signal at any given E/N) and the carrier gas used was helium, as described by Sulzer et al.[15] As both Kr^+ and O_2^+ react with picric acid via charge transfer, we have also investigated the reactions of O_2^+ with picric acid using the carrier gas (He) used in the krypton experiments to allow a direct comparison between the two studies. When operating using helium in the drift tube, the drift tube voltage is limited such that the maximum E/N that can be used is 110 Td because above this value an electrical discharge occurs, making the system unstable.

H_3O^+, NO^+, Kr^+, or O_2^+ reagent ions were produced by flowing water vapor, nitrogen/oxygen mix (3:1), krypton, or oxygen, respectively, into a hollow cathode discharge ion source. The reagent ions, under the influence of a voltage gradient, passed through a small orifice from the hollow cathode ion source into an adjacent drift (reaction) tube section, where the picric acid in trace amounts was introduced via the gas inlet system mentioned above. When using NO^+ and O_2^+ as the reagent ions, H_3O^+ was also produced owing to some residual water vapor on the surfaces of tubing going to and in the hollow cathode ion source, but this always resulted in an ion intensity of less than 5% found for that of the dominant reagent ion signal after several seconds and much less when running in pure nitrogen.

For the series of investigations presented in this study, picric acid was purchased from Sigma-Aldrich with a stated purity of ≥98%. Owing to its susceptibility to explode through friction or shock, picric acid is supplied wet, i.e., under a layer of water, which renders picric acid safe to handle. Therefore, before any measurements were taken, a small quantity of wet picric acid was placed in the glass vial and allowed to air-dry.

dx.doi.org/10.1021/jp5010192 | J. Phys. Chem. A 2014, 118, 8229−8236

Table 2. Enthalpy and Free Energy Changes for the Reactions of $PiAH^+ \cdot nH_2O$ (n = 0, 1, or 2) with H_2O at 298 K Calculated at the B3LYP 6-31+G(d,p) Level

reactants	product(s)	ΔH_{298} (kJ mol^{-1})	ΔG_{298} (kJ mol^{-1})
$PiA1H^+ + H_2O$	$PiA1H^+ \cdot H_2O$	−59	−22
$PiA1H^+ \cdot H_2O + H_2O$	$PiA1H^+ \cdot 2H_2O$	−85	−54
	$PiA + H_3O^+ \cdot H_2O$	−19	−27
$PiA1H^+ \cdot 2H_2O + H_2O$	$PiA1H^+ \cdot 3H_2O$	−86	−48
	$PiA + H_3O^+ \cdot 2H_2O$	−29	−37
$PiA4H^+ + H_2O$	$PiA4H^+ \cdot H_2O$	−97	−59
$PiA4H^+ \cdot H_2O + H_2O$	$PiA4H^+ \cdot 2H_2O$	−108	−65
	$PiA + H_3O^+ \cdot H_2O$	−34	−37
$PiA4H^+ \cdot 2H_2O + H_2O$	$PiA4H^+ \cdot 3H_2O$	−76	−44
	$PiA + H_3O^+ \cdot 2H_2O$	−21	−37

RESULTS

Electronic Structure Calculations. Since much of the thermochemistry of the reaction processes involved in this study is unknown, a series of electronic structure calculations have been undertaken. These provide crucial information which can be used to determine which reaction pathways are energetically possible. The thermochemical calculations for various reaction processes involving protonated species of importance to the study presented here are summarized in Tables 1 and 2. Table 1 presents the changes in the enthalpies and free energies for the reactions of H_3O^+, $H_3O^+ \cdot H_2O$, and $H_3O^+ \cdot 2H_2O$ with picric acid. Table 2 provides the changes in the enthalpies and free energies for the reactions of $PiAH^+ \cdot nH_2O$ (n = 0−2) with H_2O.

To our knowledge, the proton affinity of picric acid is not available in the literature. The actual value depends on which site on the picric acid the proton attaches. We have undertaken DFT calculations for the proton attaching to either the 2- or the 4-nitro groups. The calculated proton affinities corresponding to $PiA1H^+$, $PiA2H^+$, and $PiA4H^+$ are 764, 756, and 711 kJ mol^{-1}, respectively. There is only one possible structure for the 4-nitro group $PiA4H^+$ with the proton sitting on a nitro group. However, for the nitro groups adjacent to the hydroxyl group, there are two possible configurations when a proton is attached, $PiA1H^+$ and $PiA2H^+$, and these are shown in Figure 1. Transition state energies for $PiA1H^+$ to $PiA2H^+$ are calculated to be ΔH = +47 kJ mol^{-1} and ΔG = +45 kJ mol^{-1}, and it is thus likely that $PiA1H^+$ is the stable structure when the proton is transferred to the 2-nitro group. The proton affinities determined for picric acid are all greater than the proton affinity of H_2O but less than that for $(H_2O)_2$. This means that, while H_3O^+ is thermodynamically allowed to transfer a proton to picric acid, $H_3O^+ \cdot H_2O$ cannot. Ligand switching from $H_3O^+ \cdot H_2O$ to PiA to form $PiA \cdot H_3O^+$ and H_2O is thermodynamically also not possible. The value for the proton affinity corresponding to the conjugate acid $PiA4H^+$ is relatively close to water (PA(H_2O) = 691 kJ mol^{-1}).[16] On the basis of the studies of other molecules whose proton affinities are close to water, e.g., hydrogen cyanide (PA(HCN) = 713 kJ mol^{-1}) and formaldehyde (PA(HCHO) = 712 kJ mol^{-1}),[17−19] we can expect that if formed substantial back reaction of $PiA4H^+$ with water will occur owing to the large abundance of neutral water in the reaction region.

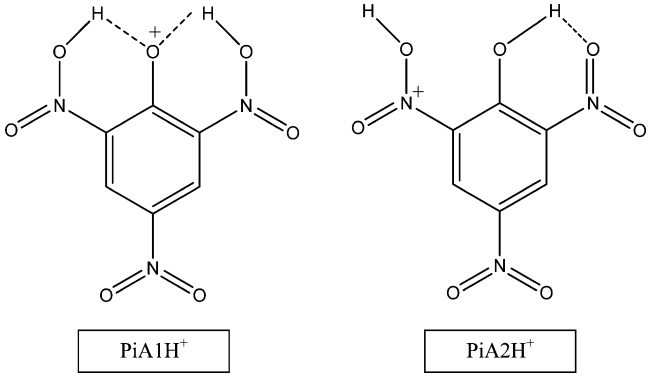

Figure 1. Structures for protonated picric acid corresponding to two possible conjugate acids.

Experimental Results. *H_3O^+ Measurements.* Figure 2a provides information on the $H_3{}^{16}O^+$ reagent ion signal (as determined in the normal way by recording the signal intensity for $H_3{}^{18}O^+$ to avoid detection saturation issues) as a function of E/N over the range 90−240 Td, as measured on the PTR-TOF 8000 instrument. The overall reagent ion signal intensity is excellent, being around 3 × 10^6 cps. However, there is an obvious dependence on intensity on E/N, which we attribute to transmission factors and, at low E/N, water clustering. Figure 2a shows that as H_3O^+ decreases at low E/N values (<120 Td) a comparable increase in $H_3O^+ \cdot H_2O$ occurs. Below approximately 100 Td, m/z 37 ($H_3O^+ \cdot H_2O$) becomes the dominant reagent ion.

Reaction of H_3O^+ with picric acid is via nondissociative proton transfer leading to $PiAH^+$. Parts b and c of Figure 2 graphically represent the dependence of the detection efficiency for $PiAH^+$ on E/N for the raw and normalized (to 10^6 H_3O^+) counts per second, respectively, using laboratory air as the carrier gas.

The E/N dependence observed for $PiAH^+$ follows a similar pattern to one we have observed for two other trinitroaromatic compounds, TNT and TNB.[3] A simple chemical mechanism explains the observations for TNT and TNB, as described briefly in the Introduction above and in more detail in ref 3. From the DFT calculations provided in Table 2, we propose a similar process is taking place with picric acid. That is, as E/N is reduced, adduct formation of $PiAH^+$ with H_2O occurs. However, we observe only small quantities of $PiAH^+ \cdot H_2O$. Therefore, as proposed for TNT and TNB, $PiAH^+ \cdot H_2O$ reacts with water, leading to the formation of PiA and $H_3O^+ \cdot H_2O$, i.e.,

$$PiAH^+ \cdot H_2O + H_2O \rightarrow H_3O^+ \cdot H_2O + PiA \quad (2)$$

The (298 K) DFT calculations show that for reaction 2 ΔG = −27 kJ mol^{-1} for $PiA1H^+$ and ΔG = −37 kJ mol^{-1} for $PiA4H^+$ (Table 2). Even if instead of reaction 1 $PiAH^+ \cdot H_2O$ forms a higher hydrate through adduct formation, the reaction of

dx.doi.org/10.1021/jp5010192 | J. Phys. Chem. A 2014, 118, 8229−8236

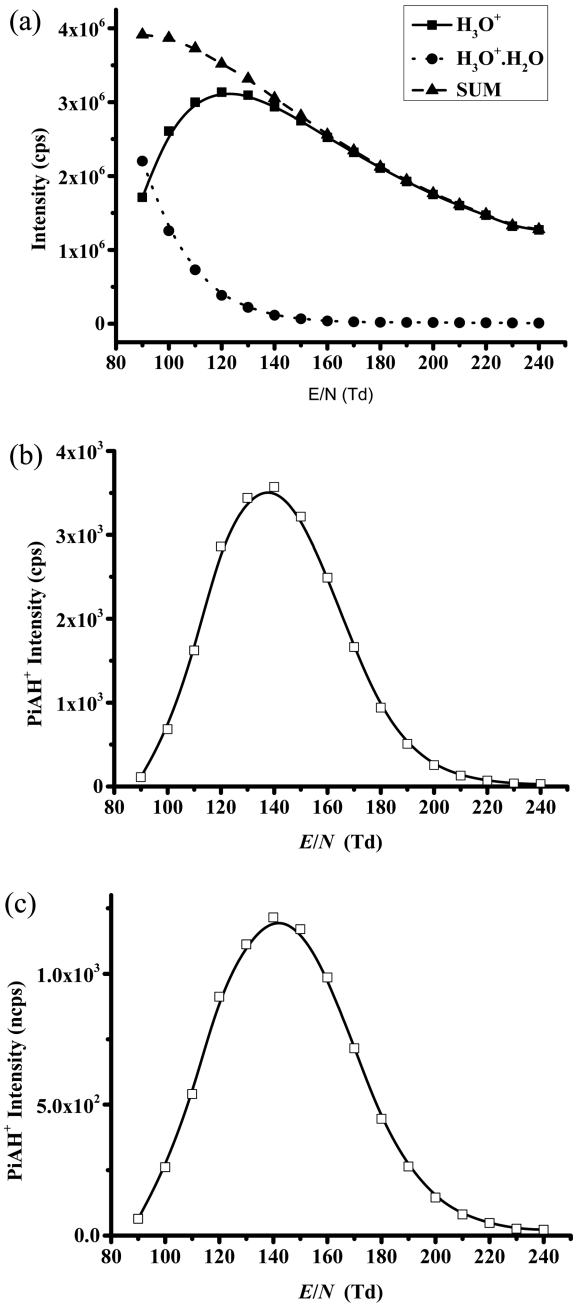

Figure 2. The variation in ion signal intensities for (a) the reagent ion H_3O^+, (b) the unnormalized protonated picric acid, and (c) the normalized (10^6 cps of H_3O^+) protonated picric acid as a function of E/N. Purified laboratory air was used as the carrier gas.

$PiAH^+ \cdot 2H_2O$ with H_2O leading to the products $H_3O^+ \cdot 2H_2O$ + PiA is also exoergonic with $\Delta G = -37$ kJ mol^{-1}. Thus, ion–molecule reactions of $PiAH^+ \cdot n(H_2O)$ with H_2O can explain the low intensity observed for the $PiAH^+ \cdot n(H_2O)$ ions and hence the reduction in the $PiAH^+$ signal at low E/N. In confirmation of this proposal, Figure 3 presents the normalized signal intensities (with the maxima set at 100 for ease of comparison) for a dry N_2 and for the case where N_2 has added water, leading to a relative humidity of 10%. (Note that, even when using N_2 as a buffer gas in the drift tube, there will still be water diffusing into the drift tube from the ion source.) In agreement with expectations, the peak intensity shifts to higher E/N as the humidity of the carrier gas in the drift tube increases.

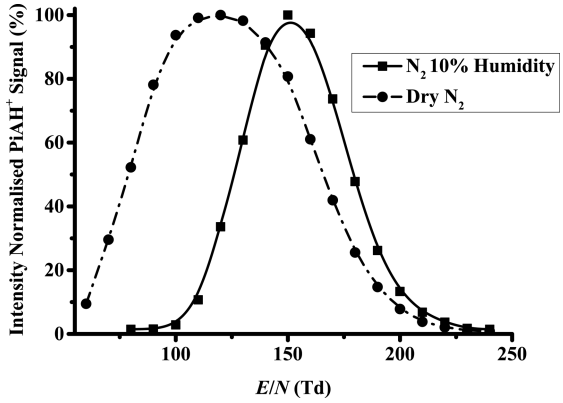

Figure 3. The relative variation in ion signal intensities for normalized $PiAH^+$ as a function of E/N using dry N_2 and N_2 at 10% humidity as carrier gases. The maximum intensity has been set at 100 for both sets of data to ease comparison.

O_2^+ Measurements. Unlike H_3O^+ studies, which are limited to E/N of greater than approximately 90 Td owing to clustering with H_2O, which dramatically reduces the H_3O^+ intensity below 90 Td (see Figure 2a), there is no such restriction for the O_2^+ measurements because there is no observable adduct formation with H_2O. Thus, for these studies, we were able to start measurements at lower E/N values. Figure 4a gives details on the O_2^+ reagent ion signal intensity as a function of E/N (60–240 Td) using laboratory air passed through a hydrocarbon trap as the buffer gas in the drift tube. This reagent ion signal had to be determined by using the molecular oxygen isotope at m/z 34 ($^{16}O^{18}O^+$), owing to detection saturation at m/z 32. It can be seen that even at 60 Td the signal intensity is relatively high at approximately 2×10^6 cps and then steadily increases as E/N increases reaching a maximum of approximately 7×10^6 cps at about 120 Td and then decreases with increasing E/N. Thus, the signal intensity of O_2^+ as a function of E/N follows a similar behavior as found for H_3O^+. Given that none of the decrease observed in the O_2^+ intensity for $E/N < 120$ Td can be attributed to cluster formation, we assume it is a result of extraction issues from the ion source. Although the change in intensity of the reagent ions over the E/N range covered in this study is not dramatic (approximately a factor of 3), it is important that any product ion signal is normalized to the reagent ion signal (we have used 10^6 cps of O_2^+).

For all E/N values, O_2^+ is found to react with picric acid by nondissociative charge transfer:

$$O_2^+ + PiA \rightarrow PiA^+ + O_2 \quad (3)$$

No other ions could be identified in the mass spectra that could be associated with the reaction of O_2^+ with PiA. For reaction 3 to be observed, the ionization potential of picric acid must be less than that of oxygen (12.07 eV). This agrees with an experimental value of the ionization potential of picric acid of 10.1 eV obtained from single photoionisation mass spectrometric measurements.[20] The dependence of PiA^+ unnormalized and normalized signal intensities as a function of E/N is shown in Figure 4b and c, respectively. We find that the PiA^+ signal intensity follows a similar dependence to that found for the $PiAH^+$ signal (although over a different E/N range). (Compare Figure 2c with Figure 4c.) To determine whether this is humidity dependent, we investigated how the peak position changes in going from using normal laboratory air to laboratory

dx.doi.org/10.1021/jp5010192 | J. Phys. Chem. A 2014, 118, 8229–8236

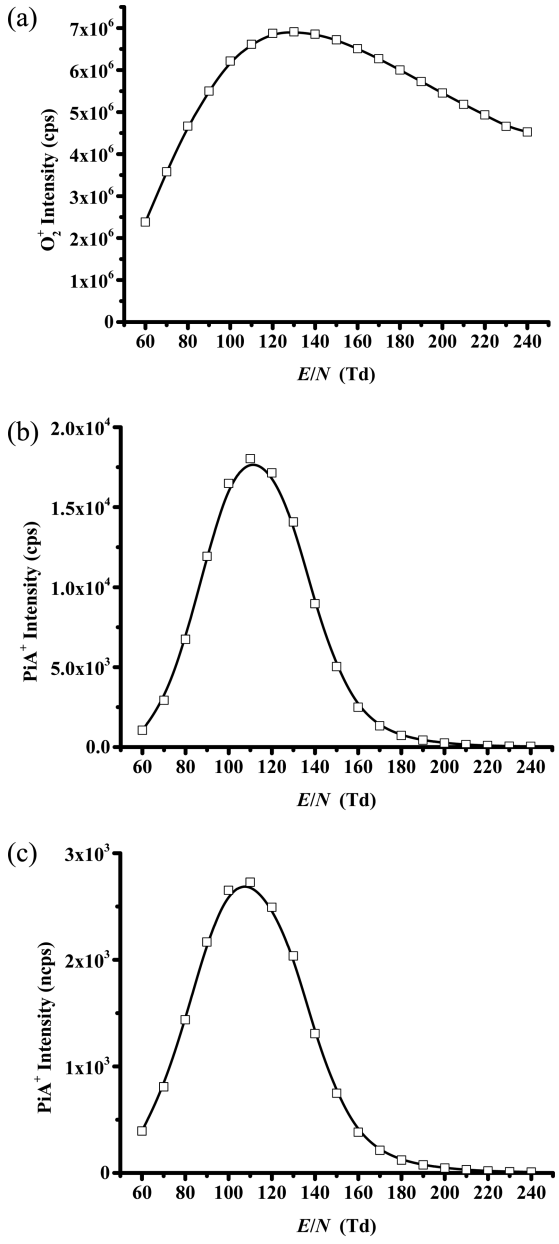

Figure 4. The variation in ion signal intensities for (a) the reagent ion O_2^+, (b) the unnormalized PiA^+, and (c) the normalized (10^6 cps of O_2^+) PiA^+ as a function of E/N. Purified laboratory air was used as the carrier gas.

air at 10% humidity. This is shown in Figure 5, which should be compared with Figure 3.

A comparison of Figures 4c and 5 with Figures 2c and 3, respectively, implies that a similar process proposed for the reaction of $PiAH^+{\cdot}H_2O$ with water (reaction 2) is occurring for $PiA^+{\cdot}H_2O$ and water, resulting in neutral PiA and a protonated water cluster:

$$PiA^+{\cdot}H_2O + H_2O \rightarrow PiA + H_3O^+{\cdot}H_2O \quad (4)$$

Table 3 presents enthalpy and free energy changes for the reactions of $PiA^+{\cdot}nH_2O$ (n = 0, 1, or 2) with H_2O at 298 K calculated at the B3LYP 6-31+G(d,p) level. From this table, it can be seen that the proposed reaction route (4) is endoergic with ΔG = +17 kJ mol^{-1}. This leads to a problem, because we have suggested in an earlier publication that an endoergicity of

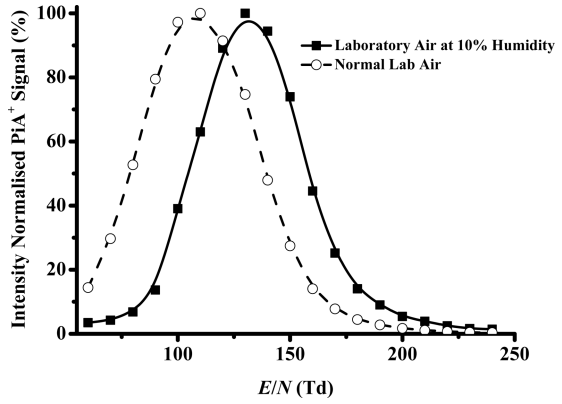

Figure 5. The variation in relative ion signal intensities for normalized PiA^+ as a function of E/N recorded using normal laboratory air compared to using laboratory air at 10% humidity as a carrier gas.

+17 kJ mol^{-1} is too high for $DNBH^+{\cdot}H_2O$ to react with water via a ligand switching mechanism within the drift tube environment.[3] However, it could be argued that PiA^+ is formed with a significant amount of internal energy following the charge transfer (approximately 2 eV), which is far more than $PiAH^+$ would have following proton transfer from H_3O^+ to DNB, and that after associating with H_2O there is sufficient energy to drive reaction 4. This raises the question as to whether excited PiA^+ would readily associate with water.

To further investigate the humidity dependence of the PiA^+ intensity, we replaced laboratory air with either pure nitrogen or helium (used also to compare later with the Kr^+ study). Parts a and b of Figure 6 show the unnormalized and normalized measurements for PiA^+ obtained when using nitrogen as the carrier gas, respectively, and Figure 7b shows the results when using He as the buffer gas. (Figure 7a shows the O_2^+ signal intensity as a function of E/N in a He buffer gas, which is considerably less than obtained when using air or nitrogen (Figure 4a) but still of sufficient intensity for our study.) It can be seen that the shape of the PiA^+ intensity curves (compare Figure 4c with Figures 6b and 7b) has dramatically changed and behaves more like the normal behavior (i.e., decreasing intensity with increasing E/N), except for an unexplained kink in the curve of Figure 6b, which approximately occurs at the position where the maximum is observed for those measurements taken using a more humid reaction chamber.

NO^+ Measurements. The NO^+ reactions with picric acid were studied to see whether they could be used for improving the selectivity. Figure 8 provides a summary of the results for the reactions of NO^+ with picric acid. As found for the production of O_2^+ reagent ions, owing to the lack of association with water, we can operate the drift tube at lower E/N values than is possible when using water vapor in the ion source. Figure 8a gives the $N^{16}O^+$ reagent ion signal intensity (calculated using the $^{15}N^{16}O^+$ signal intensity) as a function of E/N over the range 60−180 Td.

Given that the ionization potential of picric acid is greater than the recombination energy of NO^+ (9.6 eV), NO^+ reagent ions cannot react with picric acid via charge transfer processes and only adduct formation is observed ($PiA{\cdot}NO^+$). DFT calculations show that this is a strong complex (ΔG = −81 kJ mol^{-1}). However, it is only observed to be readily formed at low E/N values, as illustrated in Figure 8b and c, which give the unnormalized and normalized (to 10^6 NO^+ reagent ions per second) signal intensities, respectively, as a function of E/N.

dx.doi.org/10.1021/jp5010192 | J. Phys. Chem. A 2014, 118, 8229−8236

Table 3. Enthalpy and Free Energy Changes for the Reactions of $PiA^+ \cdot nH_2O$ (n = 0, 1, or 2) with H_2O at 298 K Calculated at the B3LYP 6-31+G(d,p) Level

reactants	product(s)	ΔH_{298} (kJ mol^{-1})	ΔG_{298} (kJ mol^{-1})
$PiA^+ + H_2O$	$PiA^+ \cdot H_2O$	−77	−43
$PiA^+ \cdot H_2O + H_2O$	$PiA^+ \cdot 2H_2O$	−90	−55
	$PiA{-}H + H_3O^+ \cdot H_2O$	+15	+17
$PiA^+ \cdot 2H_2O + H_2O$	$PiA^+ \cdot 3H_2O$	−79	−41
	$PiA{-}H + H_3O^+ \cdot 2H_2O$	+10	+8

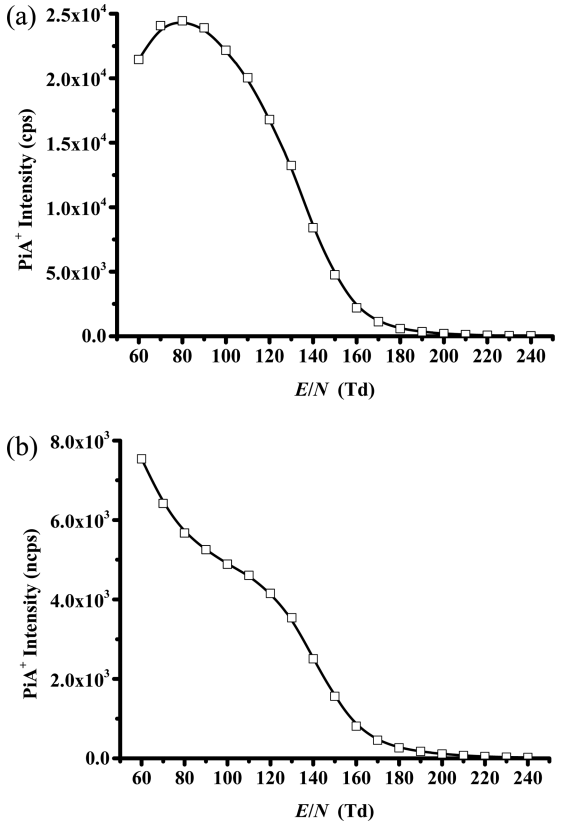

Figure 6. The variation in ion signal intensities for (a) the unnormalized PiA^+ and (b) the normalized (10^6 cps of O_2^+) PiA^+ signal intensities resulting from the reaction of O_2^+ with picric acid as a function of E/N in a "dry" reaction chamber for which high purity N_2 was used as the carrier gas.

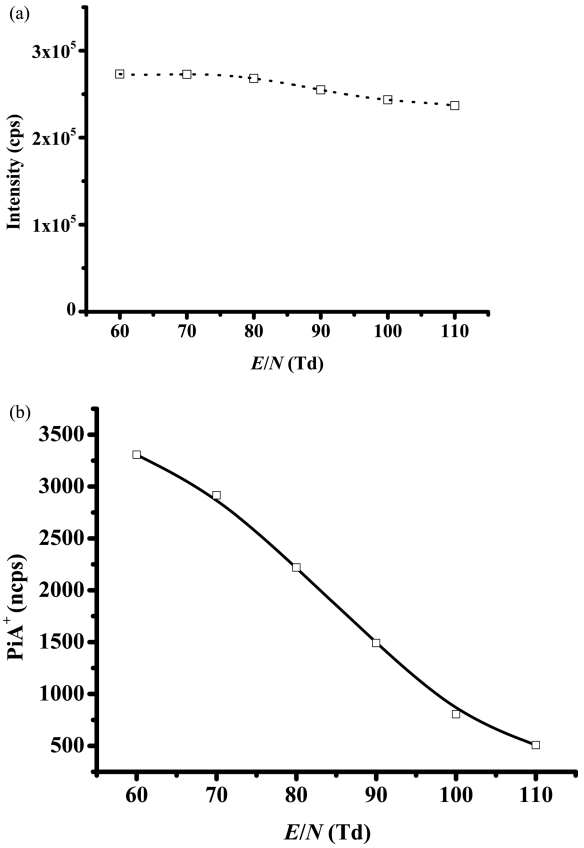

Figure 7. The variation in (a) O_2^+ ion signal intensity as a function of E/N and (b) the normalized (10^6 cps of O_2^+) PiA^+ as a function of E/N in a dry reaction chamber for which high purity He was used as the carrier gas.

Kr^+ Measurements. Figure 9a shows the total Kr^+ reagent ion signal intensity (cps) as a function of E/N over the range 60−110 Td. To determine the signal intensity, only the signal intensity at $^{78}Kr^+$ is used to determine the overall Kr^+ counts, owing to detection saturation at the m/z values corresponding to the more dominant isotopes. From Figure 9a, it can be seen that the reagent ion intensity increases with increasing E/N, starting at approximately 1.3×10^6 cps at 30 Td going up to about 3.3×10^6 cps at 110 Td. Given that Kr^+ is highly reactive, it is possible that this increase in reagent signal is associated with a reduced reaction time as E/N increases.

Kr^+ has a recombination energy of 14.0 eV, which is much higher than that for O_2^+. Therefore, we may expect that, in addition to nondissociative charge transfer, dissociative charge transfer to picric acid could occur. In agreement with this, we have observed two product ions. One is PiA^+ and the other is NO_2^+, with branching percentages of approximately 60 and 40%, respectively, across the range of E/N values investigated; i.e., there is no major E/N dependence (at 110 Td, the branching ratio of NO_2^+ has increased to about 50%). Parts b and c of Figure 9 give raw and normalized signal intensities, respectively, for PiA^+ as a function E/N. In this case, the PiA^+ follows a normal behavior of decreasing intensity with increasing E/N.

There is one final point with the Kr^+ reactions. It can be seen from Figure 9c that the maximum normalized counts per second of the product ion are significantly less than the maximum value obtained for the reactions H_3O^+ or O_2^+, although identical concentrations of picric acid in the drift tube were used for all of the experiments. This implies that the reaction efficiency is less than unity. This is entirely possible. Although exergonic proton transfer reactions generally occur with unit efficiency,[21] the same cannot be said for exergonic charge transfer processes. Factors other than energetics, such as an energy resonance connecting the neutral molecule to an ionic state at the recombination energy of the reagent ion, play a role in determining the efficiency of simple charge transfer reactions.[22]

dx.doi.org/10.1021/jp5010192 | J. Phys. Chem. A 2014, 118, 8229−8236

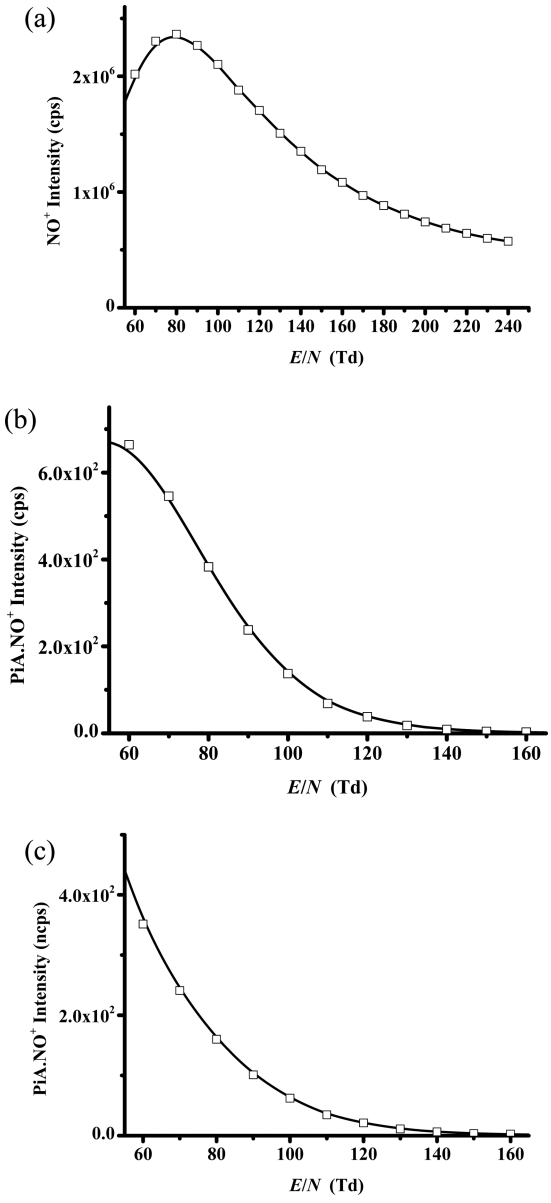

Figure 8. The variation in ion signal intensities for (a) NO^+, (b) unnormalized PiA·NO^+, and (c) normalized (10^6 cps of H_3O^+) PiA·NO^+ as a function of E/N recorded using a PTR-TOF 8000 instrument. Purified laboratory air was used as the carrier gas.

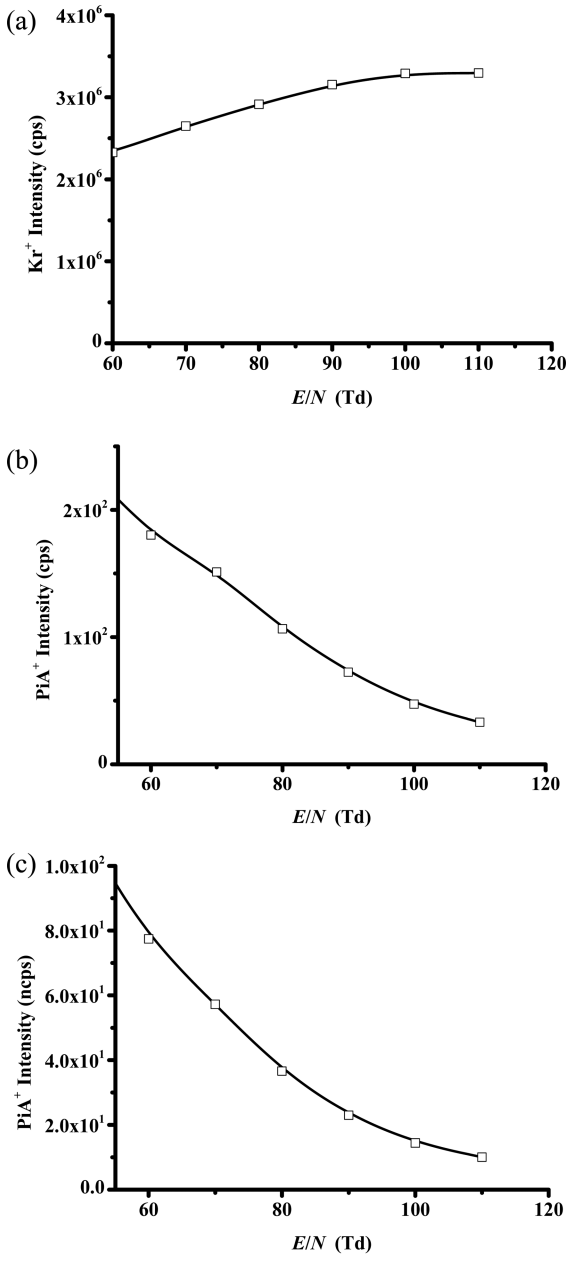

Figure 9. The variation in ion signal intensities for (a) Kr^+, (b) unnormalized PiA^+, and (c) normalized (10^6 cps of Kr^+) PiA^+ as a function of E/N recorded using a PTR-TOF 8000 instrument in an extremely "dry" reaction chamber. High purity He was used as the carrier gas.

CONCLUDING REMARKS

Using the recently developed switchable reagent ion source PTR-TOF 8000, we have investigated the reactions of H_3O^+, NO^+, O_2^+, and Kr^+ with picric acid (PiA) over a range of E/N values. The H_3O^+ investigation was undertaken to see if PiA mirrored our earlier work with TNT and TNB. The other reagent ions were investigated to see if the reaction processes lead to product ions which could be used to improve selectivity. The reaction processes are nondissociative proton transfer for reaction with H_3O^+, nondissociative charge transfer for reaction with O_2^+, nondissociative and dissociative charge transfer for reaction with Kr^+, and adduct formation for reaction with NO^+. However, the actual final product ion in a humid reaction system when either $PiAH^+$ or PiA^+ are the product ions has been found to be highly dependent on the E/N used. Once $PiAH^+·H_2O$ and $PiA^+·H_2O$ are able to be formed, we propose that secondary ion reactions with water lead to a product ion that no longer contains picric acid. As found for protonated TNT and TNB, the behavior of the intensity of protonated picric acid parent as E/N is changed by rapidly changing the drift tube voltage has the potential for use as a powerful discriminatory analytical probe to detect picric acid. This drift tube voltage bias, coupled with switching from water to oxygen chemistry, which can be done within seconds, followed again by changing E/N provides an analytical procedure for the identification of picric acid with a high level of confidence in the assignment.

For PTR-MS to be useful in security areas, special procedures need to be adopted to achieve a high level of confidence in the assignment of a compound, which is not possible just based on

dx.doi.org/10.1021/jp5010192 | J. Phys. Chem. A 2014, 118, 8229−8236

a nominal m/z value. Rapid switching of reagent ions is one way to improve selectivity. This alters the ion chemistry and hence the m/z of the product ion(s) detected. The combination of an unusual E/N dependence on ion signal intensity, which in the case of picric acid occurs for PiA^+ and $PiAH^+$ product ions, and rapid switching of reagent ions results in a powerful and multidimensional analytical tool for the screening of picric acid in complex chemical environments, providing higher confidence levels in assignment than possible when simply relying on a nominal m/z value.

AUTHOR INFORMATION

Corresponding Author

*Phone: +44 121 4144729. E-mail: c.mayhew@bham.ac.uk.

Notes

The authors declare no competing financial interest.

ACKNOWLEDGMENTS

We acknowledge the support of the PIMMS Initial Training Network which in turn is supported by the European Commission's 7th Framework Programme under Grant Agreement Number 287382.

REFERENCES

(1) Mayhew, C. A.; Sulzer, P.; Petersson, F.; Haidacher, S.; Jordan, A.; Märk, L.; Watts, P.; Märk, T. D. Applications of Proton Transfer Reaction Time-of-Flight Mass Spectrometry for the Sensitive and Rapid Real-Time Detection of Solid High Explosives. *Int. J. Mass Spectrom.* **2010**, *289*, 58−63.

(2) Jürschik, S.; Sulzer, P.; Petersson, F.; Mayhew, C. A.; Jordan, A.; Agarwal, B.; Haidacher, S.; Seehauser, H.; Becker, K.; Märk, T. D. Proton Transfer Reaction Mass Spectrometry for the Sensitive and Rapid Real-Time Detection of Solid High Explosives in Air and Water. *Anal. Bioanal. Chem.* **2010**, *398*, 2813.

(3) Sulzer, P.; Petersson, F.; Agarwal, B.; Becker, K. H.; Jürschik, S.; Märk, T. D.; Perry, D.; Watts, P.; Mayhew, C. A. Proton Transfer Reaction Mass Spectrometry and the Unambiguous Real-Time Detection of 2,4,6 TNT. *Anal. Chem.* **2012**, *84*, 4161−4166.

(4) Sulzer, P.; Jürschik, S.; Agarwal, B.; Kassebacher, T.; Hartungen, E.; Edtbauer, A.; Petersson, F.; Warmer, J.; Holl, G.; et al. Designer Drugs and Trace Explosives Detection with the Help of Very Recent Advancements in Proton-Transfer-Reaction Mass Spectrometry (PTR-MS). *Commun. Comp. Info. Sci.* **2012**, *318*, 366−375.

(5) Sulzer, P.; Agarwal, B.; Jürschik, S.; Lanza, M.; Jordan, A.; Hartungen, E.; Hanel, G.; Märk, L.; Märk, T. D.; González-Méndez, R.; et al. Applications of Switching Reagent Ions in Proton Transfer Reaction Mass Spectrometric Instruments for the Improved Selectivity of Explosive Compounds. *Int. J. Mass Spectrom.* **2013**, *354*−*355*, 123−128.

(6) Agarwal, B.; Petersson, F.; Jürschik, S.; Sulzer, P.; Jordan, A.; Märk, T. D.; Watts, P.; Mayhew, C. A. Use of Proton Transfer Reaction Time-of-Flight Mass Spectrometry for the Analytical Detection of Illicit and Controlled Prescription Drugs at Room Temperature via Direct Headspace Sampling. *Anal. Bioanal. Chem.* **2011**, *400*, 2631−2639.

(7) Jürschik, S.; Agarwal, B.; Kassebacher, T.; Sulzer, P.; Mayhew, C. A.; Märk, T. D. Rapid and Facile Detection of Four "Date Rape Drugs" in Different Beverages Utilizing Proton-Transfer-Reaction Mass Spectrometry (PTR-MS). *J. Mass Spectrom.* **2012**, *47*, 1092−1097.

(8) Lanza, M.; Acton, W. J.; Jürschik, S.; Sulzer, P.; Breiev, K.; Jordan, A.; Hartungen, E.; Hanel, G.; Märk, L.; Mayhew, C. A.; et al. Distinguishing Two Isomeric Mephedrone Substitutes with Selective Reagent Ionisation Mass Spectrometry (SRI-MS). *J. Mass Spectrom.* **2013**, *48*, 1015−1018.

(9) Acton, W. J.; Lanza, M.; Agarwal, B.; Jürschik, S.; Sulzer, P.; Breiev, K.; Jordan, A.; Hartungen, E.; Hanel, G.; Märk, L.; et al. Headspace Analysis of a Number of Designer Drugs Using a Switchable Reagent Ion Proton-Transfer-Reaction-Mass-Spectrometer. *Int. J. Mass Spectrom.* **2014**, *360*, 28−38.

(10) Petersson, F.; Sulzer, P.; Mayhew, C. A.; Watts, P.; Jordan, A.; Märk, L.; Märk, T. D. Real-Time Trace Detection and Identification of Chemical Warfare Agent Simulants using Recent Advances in Proton Transfer Reaction Time-of-Flight Mass Spectrometry. *Rapid Commun. Mass Spectrom.* **2009**, *23*, 3875−3880.

(11) Kassebacher, T.; Sulzer, P.; Jürschik, S.; Hartungen, E.; Jordan, A.; Edtbauer, A.; Feil, S.; Hanel, G.; Jaksch, S.; Märk, L.; et al. Investigations of Chemical Warfare Agents and Toxic Industrial Compounds with Proton-Transfer-Reaction Mass Spectrometry (PTR-MS) for a Real-Time Threat Monitoring Scenario. *Rapid Commun. Mass Spectrom.* **2013**, *27*, 325−332.

(12) DFT calculations were performed using the Gaussian 09 program with the GaussView interface: Frisch, M. J.; Trucks, G. W.; Schlegel, H. B.; Scuseria, G. E.; Robb, M. A.; Cheeseman, J. R.; Scalmani, G.; Barone, V.; Mennucci, B.; Petersson, G. A.; et al. *Gaussian 09*, revision A.02; Gaussian, Inc.: Wallingford, CT, 2009.

(13) http://www.ionicon.com (last accessed Jan 2014).

(14) Jordan, A.; Haidacher, S.; Hanel, G.; Hartungen, E.; Märk, L.; Seehauser, H.; Schottkowsky, R.; Sulzer, P.; Märk, T. D. A High Resolution and High Sensitivity Proton-Transfer-Reaction Time-of-Flight Mass Spectrometer (PTR-TOF-MS). *Int. J. Mass Spectrom.* **2009**, *286*, 122−128.

(15) Sulzer, P.; Edtbauer, A.; Hartungen, E.; Jürschik, S.; Jordan, A.; Hanel, G.; Feil, S.; Jaksch, S.; Märk, L.; Märk, T. D. From Conventional Proton-Transfer-Reaction Mass Spectrometry (PTR-MS) to Universal Trace Gas Analysis. *Int. J. Mass Spectrom.* **2012**, *321*−*322*, 66−70.

(16) Hunter, E. P.; Lias, S. G. "Proton Affinity Evaluation" in NIST Chemistry WebBook, NIST Standard Reference Database Number 69; Linstrom, P. J., Mallard, W. G., Eds.; National Institute of Standards and Technology: Gaithersburg, MD; http://webbook.nist.gov (accessed Jan 1, 2014).

(17) Christian, T. J.; Kleiss, B.; Yokelson, R. J.; Holzinger, R.; Crutzen, P. J.; Hao, W. M.; Shirai, T.; Blake, D. R. Comprehensive Laboratory Measurements of Biomass-Burning Emissions: 2. First Intercomparison of Open-Path FTIR, PTR-MS, and GC-MS/FID/ECD. *J. Geophys. Res.* **2004**, *109*, D02311.

(18) Karl, T. G.; Christian, T. J.; Yokelson, R. J.; Artaxo, P.; Hao, W. M.; Guenther, A. The Tropical Forest and Fire Emissions Experiment: Method Evaluation of Volatile Organic Compound Emissions Measured by PTR-MS, FTIR, and GC from Tropical Biomass Burning. *Atmos. Chem. Phys.* **2007**, *7*, 5883−5897.

(19) Knighton, W. B.; Fortner, E. C.; Midey, A. J.; Viggiano, A. A.; Herndon, S. C.; Wood, E. C.; Kolb, C. E. HCN Detection with a Proton Transfer Reaction Mass Spectrometer. *Int. J. Mass Spectrom.* **2009**, *83*, 112−121.

(20) Schramm, E.; Mühlberger, F.; Mitschke, S.; Reichardt, G.; Schulte-Ladbeck, R.; Pütz, M.; Zimmermann, R. Determination of the Ionization Potentials of Security-Relevant Substances with Single Photon Ionization Mass Spectrometry Using Synchrotron Radiation. *Appl. Spectrosc.* **2008**, *62*, 238−247.

(21) Bohme, D.; Mackay, G. I.; Schiff, H. I. Determination of Proton Affinities from the Kinetics of Proton-Transfer Reactions. VII. The Proton Affinities of O_2, H_2, Kr, O, N_2, Xe, CO_2, CH_4, N_2O and CO. *J. Chem. Phys.* **1980**, *73*, 4976−4986.

(22) Jarvis, G. K.; Kennedy, R. A.; Mayhew, C. A.; Tuckett, R. P. Charge Transfer from Neutral Perfluorocarbons to Various Cations: Long-Range Versus Short-Range Reaction Mechanisms. *Int. J. Mass Spectrom. Ion Processes* **2000**, *202*, 323−343.